Plasmon-enhanced photothermal response in heterogeneous metallic trimers

S. Toroghi[a] and P. G. Kik*[,a ,b]
[a]CREOL, The College of Optics and Photonics, University of Central Florida, 4000 Central Florida Blvd, Orlando, FL 32816, USA; [b]Department of Physics, University of Central Florida, 4000 Central Florida Blvd, Orlando, FL 32816, USA

ABSTRACT

Heat generation in plasmonic nanostructures has attracted enormous attention due to the ability of these nanostructures to generate high temperatures in nanoscale volumes using far-field irradiation, enabling applications ranging from photothermal therapy to fast (sub-nanosecond) thermal optical switching. Here we investigate the optical and thermal response of a heterogeneous trimer structure composed of a gold nanoparticle surrounded by two larger silver nanoparticles analytically and numerically. We observe that this type of multi-scale multi-material plasmonic oligomer can produce temperature changes over two orders of magnitude higher than possible with isolated gold nanoparticles.

Keywords: Cascaded plasmon resonance, Field enhancement, Heterogeneous trimer, Photothermal.

1. INTRODUCTION

The ability of metallic nanoparticles to generate heat under optical illumination is of significant interest due to the strong and localized heat dissipation that can be achieved, resulting in large temperature changes in the nanoparticles. This allows them to be used in thermally assisted applications including photothermal therapy[1,2,3,4,5], photothermal and optoacoustic imaging[6,7,8,9,10] and thermal nonlinear switching[11]. In metallic nanoparticles, absorption enhancement at the plasmon resonance frequency leads to heating of the electron gas through electron-electron scattering processes on a time scale of ~100 fs[12]. The hot electron gas in the metal nanoparticle then exchanges energy with the metal lattice through electron-phonon scattering on a picosecond time scale. Finally, over a time span of hundreds of picoseconds, heat transfer occurs from the hot metal nanoparticles to the surrounding medium. The small volume of plasmon resonant nanoparticles results in relatively rapid cooling, making them suitable candidates for observing fast thermal optical nonlinearities at relatively low irradiance.

To optimize the plasmon enhanced photothermal response, the attainable temperature change needs to be maximized for a given optical irradiance. In this study we investigate the optical and thermal response of a bimetallic trimer structure consisting of a small nanosphere with low-energy plasmon resonance between two large nanospheres with high-energy plasmon resonance. We demonstrate that the achievable relative absorption coefficient in the trimer structure can exceed that of the isolated nanoparticle by more than two orders of magnitude. Through numerical simulations we predict a temperature change of 100 K in a Ag-Au-Ag nanoparticle trimer consisting of two 80 nm diameter silver nanoparticles and a 10 nm diameter central gold nanoparticle in water shortly after a 20 nJ/mm^2 pulse at 530 nm, compared to only 0.65 K for the isolated gold nanoparticle.

2. HYBRIDIZATION MODEL

Different coupled plasmon resonances can exist in a structure with asymmetric geometry and composition which can be understood using mode hybridization theory, as shown in Figure 1. The dipolar plasmon resonance energy of isolated silver, Fig. 1(a), and gold, Fig. 1(d), embedded in water lie at 3.24 eV and 2.41 eV, respectively. Closely spaced silver and gold monomers do not interact strongly when optically excited due to the large mismatch in their plasmon resonance energies. The coupling between silver and gold nanosphere resonances can be improved by using a silver dimer structure instead of a silver monomer.

*kik@creol.ucf.edu; Phone 1 407-823-4622; Fax 1 407-823-6875

Plasmonics: Metallic Nanostructures and Their Optical Properties XII, edited by Allan D. Boardman, Proc. of SPIE Vol. 9163, 91631B · © 2014 SPIE
CCC code: 0277-786X/14/$18 · doi: 10.1117/12.2062259

The plasmon resonance of the dimer structure can be shifted to lower energy compared to that of an isolated particle due to near-field coupling for longitudinally excited nanoparticles. To illustrate this near-field mediated redshift of the resonance, Figure 1(b) schematically shows energy levels for a longitudinally excited silver dimer. The near-field interaction between two closely spaced silver nanoparticles leads to mode splitting, resulting in a low-energy bonding mode (green line) and a high-energy anti-bonding mode (black line). In the bonding mode, the electrons in both nanoparticles oscillate in-phase and the dimer structure can radiate due to the finite net dipole moment. In the anti-bonding mode, the electrons in each nanoparticle oscillate in anti-phase. The anti-bonding mode is also called dark mode due to the inability of the symmetric dimer structure to radiate, since the net dipole moment is zero. The plasmon resonance energy of the bonding mode of the silver dimer might approach the plasmon resonance energy of the gold at sufficiently small interparticle spacing. In this case, strong interactions between the silver and gold particles may be expected, since their resonance frequencies are similar. Coupling between the bonding mode of the silver dimer and the dipolar resonance of a gold monomer is expected to lead to two separate modes in a trimer structure as shown in Fig. 1(c). The lower energy mode is a bonding mode where electrons in each nanoparticle oscillate in-phase (red line). The higher energy mode is an anti-bonding mode in which the electrons in gold nanoparticle are oscillating in anti-phase compared to the electrons in the silver nanoparticles (blue line).

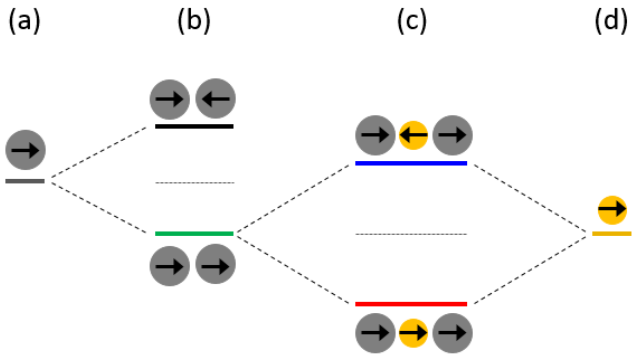

Figure 1: Energy diagrams of (a) the dipolar plasmon mode of a silver monomer, (b) the bonding (green) and anti-bonding (black) resonance modes of a silver dimer, (c) the bonding (red) and anti-bonding (blue) modes of an Ag-Au-Ag nanosphere trimer and (d) the dipolar plasmon resonance mode of a gold monomer.

3. POINT DIPOLE MODEL

A point dipole model is used to investigate the mode energies in the heterogeneous trimer structure. Each particle in the trimer is modeled as a point dipole with polarizability $\alpha_i = 3\varepsilon_0\varepsilon_h V_i(\varepsilon_m - \varepsilon_h)/(\varepsilon_m + 2\varepsilon_h)$ where V_i is the volume of nanoparticle i, and ε_m and ε_h are the dielectric function of the metal and the host, respectively. The dipole $\mathbf{p_i}$ moment of particle i is given by $\mathbf{p}_i = \alpha_i \mathbf{E}_{loc}(\mathbf{r}_i)$, where $\mathbf{E}_{loc}(\mathbf{r}_i)$ is the sum of the incident electric field $\mathbf{E}_{inc}(\mathbf{r}_i)$ and the electric fields added by neighbor dipoles at locations $\mathbf{r}_i$, leading to $\mathbf{E}_{loc}(\mathbf{r}_i) = \mathbf{E}_{inc}(\mathbf{r}_i) - \Sigma\, \mathbf{A}_{ij}\, \mathbf{p}_j$ with $\mathbf{A}_{ij}$ the dipole-dipole interaction matrix. For a linear trimer structure with two identical outer particles 1 and 3 separated by the same distance from the central particle and excited by light polarized along the trimer axis we have $\alpha_1 = \alpha_3$, $p_1 = p_3$, $A_{12}=A_{21}=A_{23}=A_{32}$ and $A_{13}=A_{31}$, where

$$A_{12} = \frac{e^{ikd}}{2\pi\varepsilon_0\varepsilon_h}\left(\frac{ik}{d_{12}^2} - \frac{1}{d_{12}^3}\right)$$
$$A_{13} = \frac{e^{ikd}}{2\pi\varepsilon_0\varepsilon_h}\left(\frac{ik}{d_{13}^2} - \frac{1}{d_{13}^3}\right) \qquad (1)$$

where d_{ij} is the center-to-center separation between particles i and j, and k is wavevector in the host medium. The dipole moment of nanoparticle i is thus given by:

$$p_i = \alpha_i\left[E_{inc} - A_{ij}p_j - A_{ik}p_k\right] \tag{2}$$

Under these assumptions the dipole moment of each nanoparticle can be found by solving the following equations:

$$\begin{aligned} p_1 = p_3 = \alpha_1 \frac{1}{1 + \alpha_1 A_{13}} \frac{1 + \alpha_1 A_{13} - \alpha_2 A_{12} - \alpha_1\alpha_2 A_{12}A_{13}}{1 + \alpha_1 A_{13} - 2\alpha_1\alpha_2 A_{12}^2} E_{inc}, \\ p_2 = \alpha_2 \frac{1 + \alpha_1 A_{13} - 2\alpha_1 A_{12}}{1 + \alpha_1 A_{13} - 2\alpha_1\alpha_2 A_{12}^2} E_{inc}. \end{aligned} \tag{3}$$

Using the frequency-dependent polarizability, α, of the individual particles as determined from their dielectric functions, the local electric field in position of each nanoparticle can be determined by $\mathbf{E}_{loc} = \mathbf{p} / \alpha$ and consequently the electric field inside the middle nanoparticle is given by

$$E_{in,2} = \frac{3\varepsilon_h}{\varepsilon_{m,2} + 2\varepsilon_h} E_{loc,2} = \frac{3\varepsilon_h}{\varepsilon_m + 2\varepsilon_h} \frac{1 + \alpha_1 A_{13} - 2\alpha_1 A_{12}}{1 + \alpha_1 A_{13} - 2\alpha_1\alpha_2 A_{12}^2} E_{inc}. \tag{4}$$

Equation 4 was used to evaluate the energy dependent field enhancement factor $|E_2/E_{inc}|$ inside the central particle in heterogeneous trimers for different monomer diameters D_2, as shown in Figure 2. For clarity the trimer is assumed to be composed of 80nm diameter outer particles with an optical response described by a Drude model with $\omega_{pA} = 9\times10^{15}$ rad/s and $\gamma_A = 1\times10^{14}$ s^{-1} and a central particle with $\omega_{pB} = 8\times10^{15}$ rad/s and $\gamma_B = 1\times10^{14}$ s^{-1}, embedded in a host with dielectric constant $\varepsilon_h = 1.77$, and at a fixed edge-to-edge separation of 5 nm between adjacent particles. The dashed gray and orange lines indicate the plasmon resonance energies of the isolated particle "A" and "B", respectively. The solid white line shows the plasmon resonance energy of the bright mode in a dimer composed of two "A" nanoparticles as a function of inter-particle spacing d_{13} in the absence of the central monomer. The field enhancement at large monomer dimer (right side of the graph) is seen to peak for low and high energy, corresponding respectively to the symmetric (bright) and anti-symmetric (dim) plasmon resonances in the trimer. The analytical resonance energy of the dimer decreases as the interparticle spacing decreases due to the aforementioned near-field interactions. The energy splitting observed in the field enhancement starts out large for large central nanoparticles, due to the relatively big influence of the large central particle on the dimer. The mode splitting decreases when the diameter of the central nanoparticle is reduced as its polarizability drops, resulting in a weaker influence of the small monomer on the dimer. Despite this reduced effect of the monomer on the dimer, the dimer does influence the response of the central particle. This is clearly seen in the achieved field enhancement values for small central particle diameter. The largest field enhancement factors are achieved when the plasmon resonance energy of the dimer matches that of the central monomer. In this low-diameter region the symmetric and anti-symmetric modes can no longer be clearly distinguished due to small mode splitting that the monomer can produce and introduction of damping related linewidth.

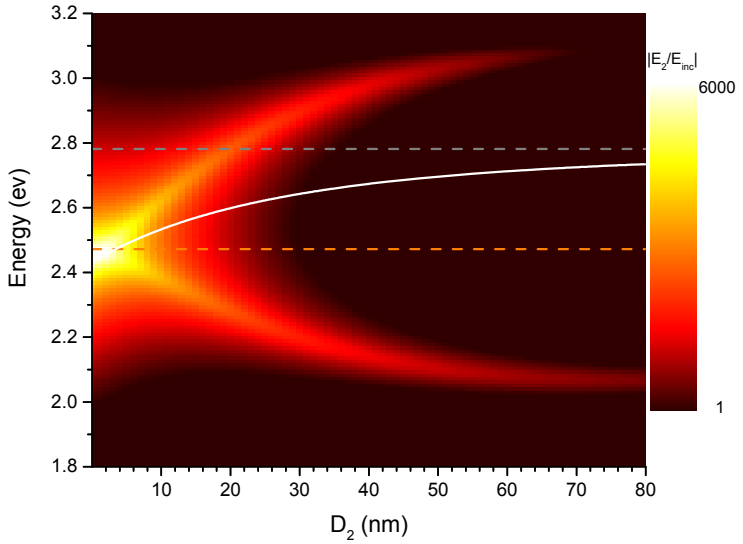

Figure 2: Internal field enhancement factor of the central nanoparticle in heterogeneous nanoparticle trimers composed of a low-loss, high plasma frequency dimer, and a high loss, low plasma frequency central nanoparticle as a function of central particle diameter D_2. (Color scale is logarithmic). The lines indicated respectively the plasmon resonance energies of isolated nanospheres composed of artificial material 'A' (dashed gray line) and 'B' (dashed orange line), and of a dimer composed of material 'A' (solid white line). The diameter of material 'A' nanoparticles is held at 80 nm.

4. FULL-FIELD SIMULATIONS

To evaluate the photothermal response that can be achieved in properly designed plasmonic trimers, electromagnetic and thermal simulations are needed. The temperature distribution inside a gold nanoparticle under illumination can be determined by:

$$\rho \cdot c_p \cdot \frac{\partial T}{\partial t} = Q + k\nabla^2 T, \tag{5}$$

where T is the time-dependent temperature distribution, and ρ, c_p and k are the density, specific heat and thermal conductivity. Q is the dissipated power density inside the gold which is the product of absorption coefficient and intensity of incident light. In the case of short pulse illumination and assuming that the heat diffusion due to the thermal conductivity is negligible, the temperature change immediately after the laser pulse is given by:

$$\Delta T = \frac{C_{abs}\,\varphi}{\rho . c_p}, \tag{6}$$

where φ is the optical fluence of the pulse and C_{abs} is relative absorption coefficient which is the ratio of the absorption cross-section to the nanoparticle volume. Equation (6) show that optimizing the relative absorption coefficient is the only way to maximize temperature change at a given optical fluence for any specific material. The relative absorption coefficient for particle i can be determined using the simulated electric field distribution as:

$$C_{abs,i} = \frac{\omega\,\varepsilon_i''}{V_i n_h c} \int_{V_i} \frac{\boldsymbol{E}^*(\boldsymbol{r}) \cdot \boldsymbol{E}(\boldsymbol{r})}{E_0^2}\, d\boldsymbol{r}. \tag{7}$$

where c is the speed of light in vacuum, n_h is the refractive index of the host, ω is angular frequency, ε_i'' is the imaginary part of the dielectric function of particle i and V_i is the volume of the nanoparticle i. $\boldsymbol{E}$ and E_0 are the enhanced and the incident electric field. Simulations based on the three-dimensional frequency domain finite integration technique were used to calculate the electric field distribution $\boldsymbol{E(r)}$ [13]. Literature data [14,15] were used for the dielectric function of gold

and silver, respectively. Figure 3 shows the simulated absorption cross-section, given by $\sigma_{abs} = C_{abs,2} \times V_2$, of a 40 nm gold nanoparticle in a heterogeneous trimer structure with a silver sphere diameter of 80 nm at 5 nm edge-to-edge spacing. The trimer was excited using plane wave illumination polarized along the trimer axis with a wavevector normal to the trimer axis. The absorption cross-section spectrum shows a peak at 570 nm and a shoulder approximately around 510 nm. To investigate the nature of these modes, Figs. 3(b) and 3(c) show the field distribution at a wavelength of 570 nm and 510 nm, respectively. As expected based on the hybridization model shown in Fig. 1, the low frequency mode indeed shows that the field inside the gold nanoparticle and silver nanoparticles are in the same direction. In other words, the dipole moment of the gold nanoparticle oscillates in-phase with the dipole moment of the two silver nanoparticles, indicative of a bonding mode. The high-frequency mode on the other hand shows that the field inside the gold nanoparticle is in opposite direction compared to that inside the silver nanoparticles, i.e. the dipole moment of the gold monomer oscillates in anti-phase with that of the silver nanoparticles, indicative of an anti-bonding mode. For reference, the location of the isolated gold nanoparticle plasmon resonance is indicated by the dashed line in Fig. 3(a). Note that the gold monomer resonance lies in between the bonding and anti-bonding modes, as expected based on the analysis in Fig. 1.

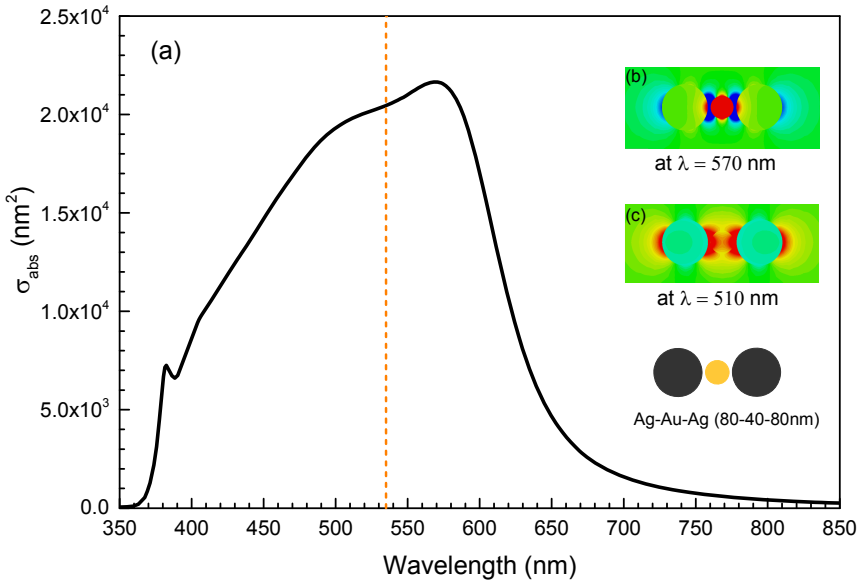

Figure 3: (a) Absorption cross-section of a gold nanoparticle in a trimer structure consisting of two 80 nm silver nanoparticles and a 40nm gold nanoparticle. The edge-to-edge spacing between each nanoparticle is 5nm. The dashed line shows the isolated gold nanoparticle resonance. Distribution of the electric field (longitudinal component) at a wavelength of (b) 570 nm and (c) 510 nm.

Figure 4 shows the simulated relative absorption coefficient C_{abs} for three different sizes of the gold nanospheres in the multi- material trimer structure (solid lines) and in the monomer structure (dotted lines). The relative absorption coefficient of a trimer with a 80 nm gold nanoparticle, red solid line, shows peaks at 495 nm and at 675 nm. A trimer with a 40 nm gold nanosphere shows a higher relative absorption coefficient, green solid line, compared to the 80 nm nanosphere case. The spectrum shows a peak at 570 nm and a shoulder at approximately 510 nm. Finally, the relative gold related absorption coefficient of a trimer with a 10 nm gold nanosphere, blue solid line, shows one peak at 530 nm. The relative absorption coefficient values for three different isolated gold nanoparticles with these sizes, dotted lines, show a small shift in peak position due to phase retardation effects, and are two orders of magnitude smaller than that for a 10nm gold nanoparticle in the trimer structure. The relative absorption coefficient can be related directly to the temperature change in the nanoparticles as shown in equation (6). The related temperature change for a 10 nm gold nanoparticle in trimer structure in water shortly after a 20 nJ/mm^2 pulse at 530 nm is 100 K which is more than two orders of magnitude larger than that for the isolated gold nanoparticle (0.65 K).

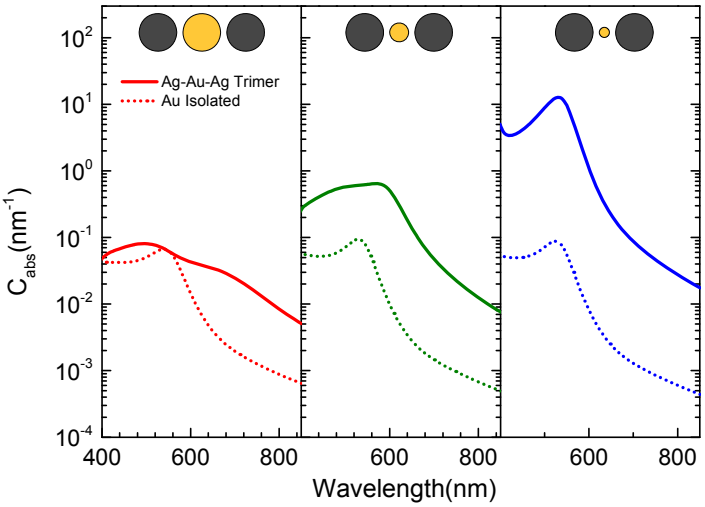

Figure 4: Relative absorption coefficient for gold nanospheres with size of 80 nm in heterogeneous trimer structure (red solid line) and monomer structure (red dotted line), with size of 40 nm in heterogeneous trimer structure (green solid line) and monomer structure (green dotted line), and with size of 10 nm in heterogeneous trimer structure (blue solid line) and monomer structure (blue dotted line). Trimer structure consists two 80 nm diameter outer silver nanoparticles.

The results show the relative absorption coefficient can be enhanced by more than two orders of magnitude using carefully engineered coupled resonances in heterogeneous trimer structures. This enhanced and localized energy absorption in the gold nanoparticle can lead to a rapid temperature changes inside gold nanoparticle and in the particle's vicinity in the host medium. The fast and large temperature changes in the gold nanoparticle are expected to lead to significantly enhanced thermal nonlinear optical response through the photothermal effect. The spherical particle shape is expected to make these structures thermodynamically stable up to relatively high temperatures. The particle sizes and the gap sizes used can be achieved using chemical synthesis methods such as surface-charge based binding or with short organic linker molecules.

5. CONCLUSIONS

The optical and thermal response of a gold nanoparticle placed between two larger silver nanoparticles have been investigated. It was shown through numerical simulation that a temperature change of 100 K can be achieved in a Ag-Au-Ag nanoparticle trimer consisting of two 80 nm diameter silver nanoparticles and a 10 nm diameter central gold nanoparticle in water shortly after a 20 nJ/mm^2 pulse at 530 nm, compared to only 0.65 K for an isolated gold nanoparticle of the same size. This effect could be understood in terms of the hybridization of the silver dimer plasmon resonance and the gold nanoparticle resonance. The predicted effects can be achieved using experimentally realizable particle sizes.

REFERENCES

[1] Lal, S.; Clare, S. E.; Halas, N. J., "Nanoshell-Enabled Photothermal Cancer Therapy: Impending Clinical Impact," Accounts Chem Res 41(12), 1842-1851 (2008).
[2] Huang, X. H.; Jain, P. K.; El-Sayed, I. H.; El-Sayed, M. A., "Plasmonic photothermal therapy (PPTT) using gold nanoparticles," Laser Med Sci 23(3), 217-228 (2008).
[3] Pitsillides, C. M.; Joe, E. K.; Wei, X. B.; Anderson, R. R.; Lin, C. P., "Selective cell targeting with light-absorbing microparticles and nanoparticles," Biophys J 84(6), 4023-4032 (2003).
[4] Lapotko, D.; Lukianova, E.; Potapnev, M.; Aleinikova, O.; Oraevsky, A., "Method of laser activated nano-thermolysis for elimination of tumor cells," Cancer Lett 239(1), 36-45 (2006).

[5] Loo, C.; Lowery, A.; Halas, N. J.; West, J.; Drezek, R., "Immunotargeted nanoshells for integrated cancer imaging and therapy," Nano Lett 5(4), 709-711 (2005).
[6] Boyer, D.; Tamarat, P.; Maali, A.; Lounis, B.; Orrit, M., "Photothermal imaging of nanometer-sized metal particles among scatterers," Science 297(5584), 1160-1163 (2002).
[7] Cognet, L.; Tardin, C.; Boyer, D.; Choquet, D.; Tamarat, P.; Lounis, B., "Single metallic nanoparticle imaging for protein detection in cells," P Natl Acad Sci USA 100(20), 11350-11355 (2003).
[8] Cognet, L.; Berciaud, S.; Lasne, D.; Lounis, B., "Photothermal methods for single nonluminescent nano-objects," Anal Chem 80(7), 2288-2294 (2008).
[9] Copland, J. A.; Eghtedari, M.; Popov, V. L.; Kotov, N.; Mamedova, N.; Motamedi, M.; Oraevsky, A. A., "Bioconjugated gold nanoparticles as a molecular based contrast agent: Implications for imaging of deep tumors using optoacoustic tomography," Mol Imaging Biol 6(5), 341-349 (2004).
[10] Mallidi, S.; Larson, T.; Aaron, J.; Sokolov, K.; Emelianov, S., "Molecular specific optoacoustic imaging with plasmonic nanoparticles," Opt Express 15(11), 6583-6588 (2007).
[11] Nielsen, M. G.; Bernardin, T.; Hassan, K.; Kriezis, E. E.; Weeber, J. C., "Silicon-loaded surface plasmon polariton waveguides for nanosecond thermo-optical switching," Opt Lett 39(8), 2282-2285 (2014).
[12] Puech, K.; Henari, F. Z.; Blau, W. J.; Duff, D.; Schmid, G., "Investigation of the Ultrafast Dephasing Time of Gold Nanoparticles Using Incoherent-Light," Chem Phys Lett 247(1-2), 13-17 (1995).
[13] "Microwave Studio, Computer Simulation Technology, Darmstadt, Germany," (2013).
[14] Johnson, P. B.; Christy, R. W., "OPTICAL CONSTANTS OF NOBLE METALS," Physical Review B 6(12), 4370-4379 (1972).
[15] Toroghi, S.; Kik, P. G., "Cascaded plasmonic metamaterials for phase-controlled enhancement of nonlinear absorption and refraction," Physical Review B 85(4), 045432 (2012).